NAVAL POSTGRADUATE SCHOOL
Monterey, California

THESIS

ANALYSIS OF ACOUSTIC PLANE-WAVE VARIABILITY IN THE REGION OF THE MID-ATLANTIC BIGHT SHELF BREAK

by

Jerry L. Sullivan

December 1997

Thesis Advisor: Kevin B. Smith

Approved for public release; distribution is unlimited.

REPORT DOCUMENTATION PAGE

Form Approved OMB No. 0704-0188

1. AGENCY USE ONLY *(Leave blank)*	2. REPORT DATE	3. REPORT TYPE AND DATES COVERED
	December 1997	Master's Thesis

4. TITLE AND SUBTITLE
ANALYSIS OF ACOUSTIC PLANE-WAVE VARIABILITY IN THE REGION OF THE MID-ATLANTIC BIGHT SHELF BREAK

5. FUNDING NUMBERS

6. AUTHOR(S)
Jerry L. Sullivan

7. PERFORMING ORGANIZATION NAME(S) AND ADDRESS(ES)
Naval Postgraduate School
Monterey, CA 93943-5000

8. PERFORMING ORGANIZATION REPORT NUMBER

9. SPONSORING / MONITORING AGENCY NAME(S) AND ADDRESS(ES)

10. SPONSORING / MONITORING AGENCY REPORT NUMBER

11. SUPPLEMENTARY NOTES
The views expressed in this thesis are those of the author and do not reflect the official policy or position of the Department of Defense or the U.S. Government.

12a. DISTRIBUTION / AVAILABILITY STATEMENT
Approved for public release; distribution is unlimited.

12b. DISTRIBUTION CODE

13. ABSTRACT *(maximum 200 words)*

From the summer cruise of the Mid-Atlantic Bight Experiment, conducted jointly by Naval Postgraduate School, University of Rhode Island, and Woods Hole Oceanographic Institution, a study of acoustic variability in the region of Mid-Atlantic Bight shelf break was conducted. The period of the experiment was 19 July to 09 August 1996. The experiment consisted of a suite of acoustic and oceanographic sensors including three 400 Hz (100 Hz bandwidth) transceivers, one 224 Hz (16 Hz bandwidth) transceiver and two vertical line arrays (VLAs). This study involves the signal processing of data collected by a telemetry buoy, an analysis of the spatial and temporal coherence of the phones and plane-wave beams of the vertical array, and the tidal and seasonal variabilities of plane-wave arrivals at the vertical array. Results of the changes in arrival time of the beams, the horizontal displacement of the front, the changes in the speed of propagation of the wave, and the change in the water temperature are discussed.

14. SUBJECT TERMS	15. NUMBER OF PAGES
Mid-Atlantic Bight plane-wave beamforming temporal coherence spatial signal processing shelf front tidal response ocean acoustics	56
	16. PRICE CODE

17. SECURITY CLASSIFICATION OF REPORT	18. SECURITY CLASSIFICATION OF THIS PAGE	19. SECURITY CLASSIFI- CATION OF ABSTRACT	20. LIMITATION OF ABSTRACT
Unclassified	Unclassified	Unclassified	UL

NSN 7540-01-280-5500

Standard Form 298 (Rev. 2-89)

Prescribed by ANSI Std. 239-18 298-102

Approved for public release; distribution is unlimited

ANALYSIS OF ACOUSTIC PLANE-WAVE VARIABILITY IN THE REGION OF THE MID-ATLANTIC BIGHT SHELF BREAK

Jerry L. Sullivan
Lieutenant, United States Navy
B.S., Southern University A&M, 1990

Submitted in partial fulfillment of the
requirements for the degree of

MASTER OF SCIENCE IN APPLIED PHYSICS

from the

NAVAL POSTGRADUATE SCHOOL
December 1997

Author: _____
Jerry L. Sullivan

Approved by: _____
Kevin B. Smith, Thesis Advisor

_____
James V. Sanders, Second Reader

_____
William B. Maier II Chairman
Department of Physics

ABSTRACT

From the summer cruise of the Mid-Atlantic Bight Experiment, conducted jointly by Naval Postgraduate School, University of Rhode Island, and Woods Hole Oceanographic Institution, a study of acoustic variability in the region of Mid-Atlantic Bight shelf break was conducted. The period of the experiment was from 19 July to 09 August 1996. The experiment consisted of a suite of acoustic and oceanographic sensors including three 400 Hz (100 Hz bandwidth) transceivers, one 224 Hz (16 Hz bandwidth) transceiver and two vertical line arrays (VLAs). This study involves the signal processing of data collected by a telemetry buoy, an analysis of the spatial and temporal coherence of the phones and plane-wave beams of the vertical array, and the tidal and seasonal variabilities of plane-wave arrivals at the vertical array. Results of the changes in arrival time of the beams, the horizontal displacement of the front, the changes in the speed of propagation of the wave, and the change in the water temperature are discussed.

TABLE OF CONTENTS

ACKNOWLEDGEMENTS

I would like to take this opportunity to acknowledge those people to have helped me throughout this thesis process. First, I would like to thank my thesis advisor, Professor Kevin B. Smith for his guidance, enlightenment, and instruction during the whole ordeal. Kevin could always enlighten me on the subject at hand. Furthermore, without Kevin, this thesis could not have been completed.

Next, I would like to thank Chris Miller, COACT lab supervisor, for all of his help. Chris was an expert on every question and every problem that arose. Thanks, also to Rob Bourke for his enthusiasm and quick response to hardware and software failures. A special thank you goes to Ms. Sandra Lackey for her expertise in word processing.

Thirdly, I would thank my colleagues "underwater acoustics study group": LT A. Bettega, LCDR J. Brune, CDR J. Rojas for their . These guys came to my aid on many occasions, when I was overwhelmed with the work of this thesis.

Then, I would like to thank my wife, Regina, for her unwavering support and tireless effort in the caring of our four children, Jerry II, Jeron, Jeremy, and Reona. Regina had to respond very quickly to my challenging schedule after giving birth to our daughter, Reona, in my final quarter of study.

Finally, I thank my Heavenly Father for His immeasurable grace that he has bestowed upon us.

I. INTRODUCTION

A. OBJECTIVES OF THE MID-ATLANTIC BIGHT EXPERIMENT

The end of the Cold War and the operations in Desert Storm have brought about new challenges in undersea warfare (USW). The mission of USW is "battlespace dominance in support of Forward From The Sea" (Snyder, 1997). Navy systems must be technologically advanced and highly efficient in diverse littoral regions. To operate effectively, the Navy must perform research in these littoral regions. To meet this objective, the Mid-Atlantic Bight (MAB) experiment was conducted. The overall scientific goal of the MAB experiment was to quantify shelfbreak frontal variability and its coupling to adjacent slope water circulation and to determine the impact of this variability on sound propagation from the continental slope onto the shelf (Smith et al., 1996). The MAB experiment also focuses on determining temperature structure of the ocean environment via acoustic tomography. It will use the two aspects of tomography: the forward problem and the inverse problem. The forward problem emphasizes the forward propagation modeling and the generation of replicas to determine the limitations on how replicas affect tomographic methods. The inverse problem utilizes replicas to localize the environmental parameters. Furthermore, the MAB experiment has cultivated the study in the area of geo-

acoustic inversions - extraction of bottom sound speed and density from data - and horizontal refraction (3-D effects). A secondary goal of the Mid-Atlantic Bight experiment is to obtain sufficient oceanographic and acoustical data to be able to contrast the wintertime and summertime variability of the shelfbreak front (Smith et al., 1996). The gain that the Navy gets from this study is fundamental insights into acoustic propagation in the slope-shelf transition region and application of these insights to target detection and localization.

B. THESIS OBJECTIVES

The objectives of this study are as follows.

1. Adapt signal processing algorithms to the real acoustical environment in order to process three days of real continuous vertical line array (VLA) data.
2. Quantify the variabilities of plane wave arrivals and compare these variabilities with expected variations in the environment.
3. Analyze the spatial and temporal coherence of the phones and beams of the vertical array.
4. Determine whether the variabilities are due to nonlinear solitons passing through the region or larger scale frontal variability.

II. OVERVIEW OF MID-ATLANTIC BIGHT EXPERIMENT

The Mid-Atlantic Bight experiment (a combined oceanographic and acoustic experiment) was conducted jointly by the Naval Postgraduate School, the University of Rhode Island, and the Woods Hole Oceanographic Institution. The location of the experiment is the region of the continental shelf break south of Cape Cod.

The Mid-Atlantic Bight experiment consisted of two cruises - a summer cruise (19 July to 9 August 1996) and winter cruise (09 February to 27 February 1997). The summer and winter cruises were proposed to compare summertime and wintertime variation of the shelf break fronts. This study will focus on the summer cruise. The summer cruise was aboard the R/V *Endeavor* from the University of Rhode Island. Major operations involved on the cruise were equipment deployment, operations of the Seasor, and hydrography. During the time of the experiment, the nature of the region was complex. The front was distorted by an eddy filament which was produced by a warm core ring absorbed by the Gulf Stream and the shelf water was moving soutwest (Pickart et al., 1996)

The acoustical elements of this cruise were three 400 Hz sources (100 Hz bandwidth), one 224 Hz source (16 Hz bandwidth), two 16 element vertical line arrays (VLA) or "tomography" arrays and one physical oceanographic array.

The location of each acoustic element is listed in Table 1. The arrangement of the acoustical elements is illustrated in Fig. 1. In Fig. 1, the two northern most triangles are the VLA's, the three triangles to the south are the three 400 Hz sources. It is seen that the 400 Hz sources are on the seaward side transmitting to two VLA's on the shoreward side. The concentration of this paper will be on the data received at the northwest (NW) VLA from the southwest (SW) 400 Hz source at 300 meter depth.

Acoustical Element	Latitude	Longitude	Water Depth (m)	Dist to NW VLA (km)
NW VLA	40° 22.310′	71° 13.478′	87	0
224 Hz	40° 00.065′	71° 09.702′	296	41.0
400 Hz	40° 00.007′	71° 10.083′	300	41.0
400 Hz	40° 00.000′	71° 44.495′	285	58.0
400 Hz	39° 56.003′	70° 55.487′	472	55.0

Table 1: Acoustic mooring locations for Mid-Atlantic Bight experiment.

The Seasor is a towed mechanical fish provided by the Woods Hole Oceanographic Institution. Towed in a "yo-yo" manner behind the R/V *Endeavor*, it provided information on the water column properties during the experiment, including temperature and salinity as a function of depth. This data was later converted into sound speed profiles as shown in Fig. 2. This figure displays one data set taken along the

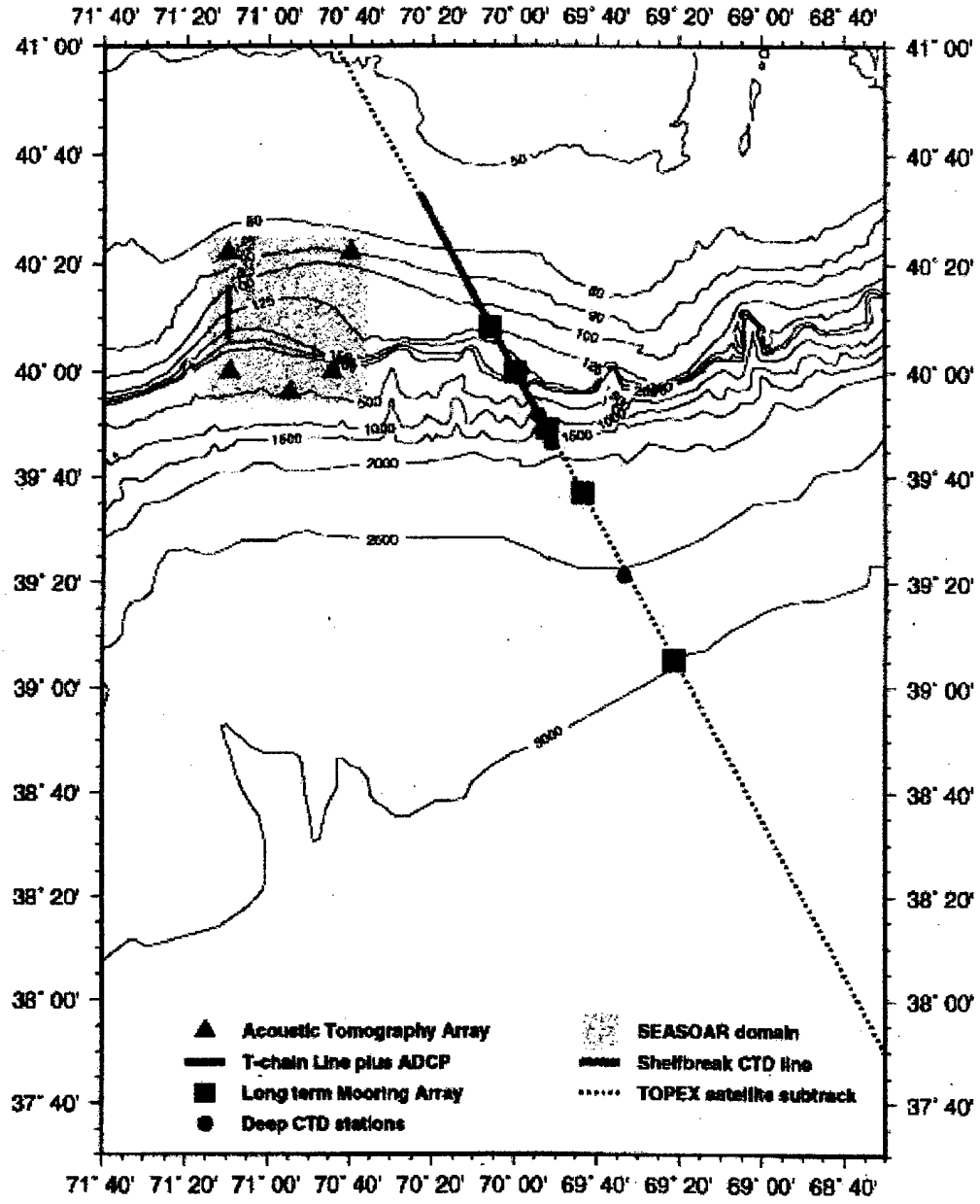

Figure 1: Arrangement of acoustical elements of the Mid-Atlantic Bight experiment.

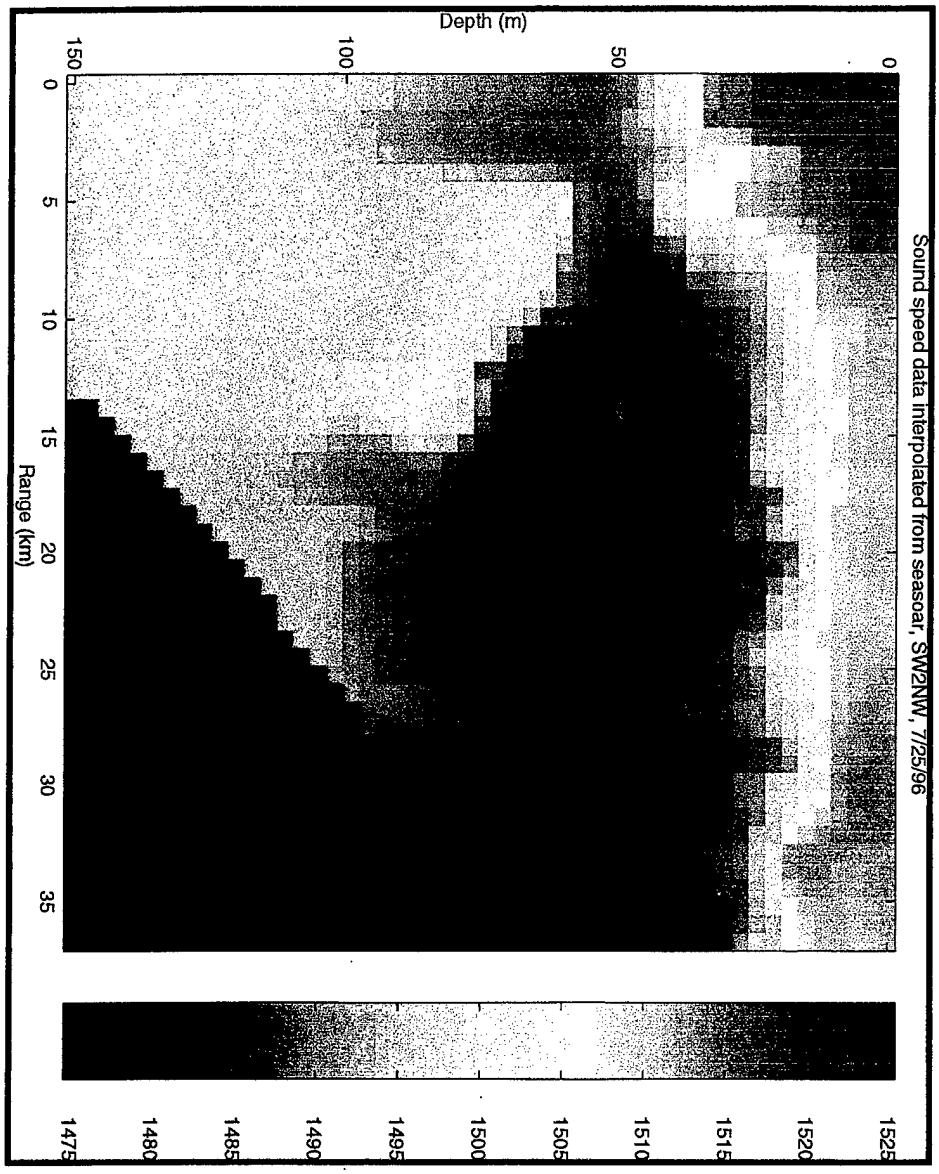

Figure 2: Sound speed profile generated from Seasoar data collected during the MAB experiment (units of sound speed in m/s).

track of interest in this study. The low sound speeds on the shelf are indicative of the cold water typical on northern latitude shelf regions. The strong shelf break front, from cold water to warm water, is also a characteristic feature of some shelf break environments. This large-scale front is expected to have a considerable influence on the acoustic propagation in the region and is one of the key features to be studied.

III. NUMERICAL METHODS AND SIGNAL PROCESSING

A. MATCHED-FILTER PROCESSING

To obtain adequate signal-to-noise ratio (SNR) without losing resolution, modulated signals were transmitted extending the signal duration without reducing bandwidth. To correlate the received signal, a process known as matched-filtering is performed. The modulation of the signal must be such that the autocorrelation of the received signal will be much shorter than the transmitted signal. The matched-filter process is based on the assumption that the ocean sound channel can be modeled as a linear, time-invariant system. Based on this assumption, the received signal is the sum of delayed replicas of the transmitted signal (Munk et al., 1995),

$$r(t) = \sum_j k_j s(t - T_j) \tag{3.1}$$

where r(t) is the received signal, k_j is the amplitude of j^{th} ray, s(t) is the transmitted signal, and T_j is the travel time of the j^{th} ray. The output of the matched-filter is given by

$$p(\tau) = \int r(t)\, s^*(t - \tau) dt, \tag{3.2}$$

where $p(\tau)$ is the output of the received signal after applying a matched-filter. The autocorrelation of Eq. (3.2) yields (Clay and Medwin, 1977)

$$p(\tau) = \int P(f) e^{i2\pi f\tau} df \tag{3.3}$$

where P(f) is the product of S*(f)and R(f), the transmitted and received signal respectively, in the frequency domain.

The matched-filter process, in general, correlates the received signal with a replica of the transmitted signal. The matched-filtering technique used to process the data from the Mid-Atlantic Bight experiment is a technique introduced by Birdsall and Metzger (1986). Birdsall and Metzger pioneered the idea of phase encoding a signal using binary finite-field algebraic codes (also known as m-sequences). Using m-sequencing, a phase encoded signal can be written as

$$r(t) = Z\cos(\omega_o t + M(t)\phi_o) \tag{3.4}$$

where r(t) is the phase encoded signal, Z is the amplitude of the signal, ω_0 is the carrier frequency, M(t) is the m-sequence to be encoded and ϕ_0 is the phase angle. The complex envelope of Eq. (3.4) is

$$\hat{s}(t) = Be^{iM(t)\phi_0} \tag{3.5}$$

where B is the amplitude of the signal. The autocorrelation is written as

$$r(\tau) = \int Be^{iM(t)\phi_0} Be^{-iM(t+\tau)\phi_0} d\tau. \tag{3.6}$$

The acoustic signals of the MAB experiment consist of 10 millisecond pulse transmissions. These transmissions were matched-filtered and coherently averaged over five minutes. They were then stored as transmission records at an interval of fifteen minutes. The fifteen-minute interval includes five minutes of transmitting and ten minutes of silence. An example of a transmission record is displayed in Fig. 3 as a depth-time plot. The phones are numbered vertically from top to bottom. The phone locations are from 31.5 to 84 meters in depth every 3.5 meters for a total of 16 phones. The red region indicates the highest energy of the arrivals.

B. PLANE-WAVE BEAMFORMING

After an acoustic signal has been received, there are a variety of techniques available to distinguish a particular feature of the propagation as well as reduce the influence of noise on the signal. Noise is usually generated near the surface and tends to occur in high modes or high angles of propagation (Jensen et al., 1994). Plane-wave beamforming is a process that involves decomposing a signal

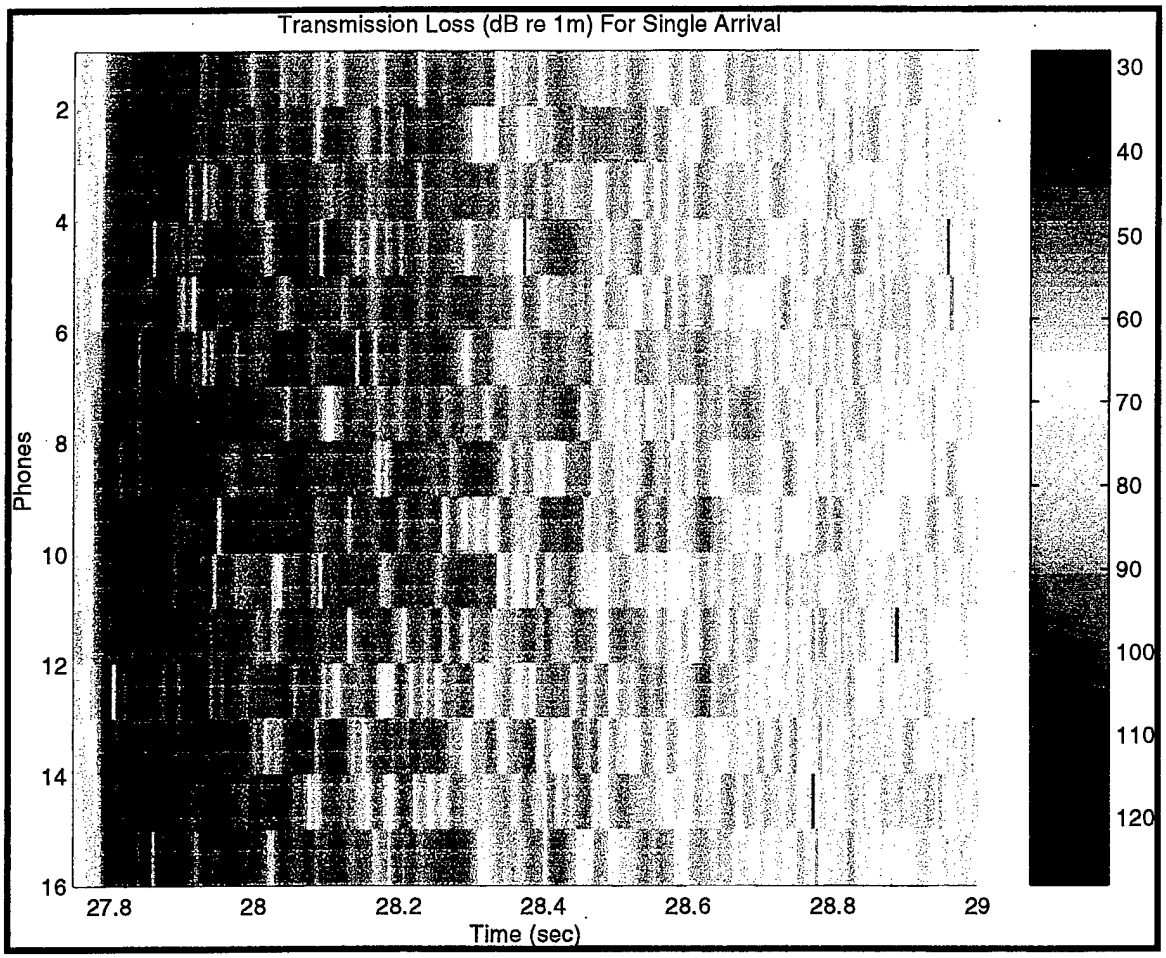

Figure 3: Depth-time plot of a single transmission from the SW 400 Hz source measured at the NW VLA.

into plane waves. This application is especially useful in underwater acoustics because the propagation of acoustic waves and the source/receiver locations are contained in the vertical structure of the acoustic field. Although the arrivals at the VLA will not simply be plane waves due to the variation in sound speed across the array, these variations are less than 2% and will be ignored here.

Summing the outputs of spatially distributed sensors defines the concept of beamforming. A beamformer's output is far more useful than an individual sensor for it allows one to listen preferentially to wavefronts propagating from one direction over another. Therefore, a beamformer implements a spatial filter. For example, Defatta et al. (1988) describe beamforming using a line array of equally spaced elements. Let the position of each element be along the z-axis in an infinite, homogeneous medium with an undetermined number of remote sources. Then the output of an element at the origin of the coordinate system from the m^{th} source is $s_m(t)$. From the far-field plane-wave approximation, a source from direction θ_l produces outputs of the form

$$f_l(t) = s_m\left(t + \frac{ld\sin(\theta_m)}{c}\right), \tag{3.7}$$

where l is the array element index, d is the spacing of the elements, θ_m is the angle of arrival from the m^{th} source, and

c is the speed of propagation. To accomplish beamforming, one must apply weights and time delays to the individual element signals and then sum them coherently. The output of the beamformer in the direction θ_n is then

$$b_n(t) = \sum_{l=1}^{L} w_l s_m\left(t + \frac{ld\left(\sin(\theta_m) - \sin(\theta_n)\right)}{c}\right), \tag{3.8}$$

where w_l are the element signal weights.

To derive the directional response characteristics of the beamformer, consider a continuous, complex, plane-wave signal propagating across the array, defined by

$$s_m(t) = e^{i\omega_m t}. \tag{3.9}$$

Because of the angle of arrival, θ_m, the source produces outputs of the form

$$e_l(t) = e^{i\omega_m t} e^{ilk_m d \sin(\theta_m)}, \tag{3.10}$$

where $k_m = \frac{2\pi}{\lambda_m} = \frac{\omega_m}{c}$ is the wavenumber of the m^{th} source. The beamformer output is then

$$b_n(t) = e^{i\omega_m t} \sum_{m=1}^{M} w_m e^{-imk_m d\left[\sin(\theta_n) - \sin(\theta_m)\right]} W(\theta_m), \tag{3.11}$$

where

$$W(\theta_m) = \sum_{l=1}^{L} w_L e^{-il k_m d(\sin(\theta_n)-\sin(\theta_m)} \tag{3.12}$$

is the spatial Fourier transform of the array weights (Defatta et al., 1988).

For all of the beamforming shown in this thesis, a beamforming program written in matlab was used. The program was tested on model data of known characteristics before being used on real data. Comparisons of real beamformed data and model predictions were also made.

1. Predicted Arrival Structures

To predict the arrival structure of the acoustical beams, the Monterey-Miami Parabolic Equation (MMPE) model was used. This model, formerly known as the University of Miami Parabolic Equation (UMPE) model (Smith and Tappert, 1995), uses the parabolic approximation method with a split-step Fourier algorithm (Hardin and Tappert, 1973) to solve the acoustic wave equation in cylindrical coordinates. Selected outputs generated by the model are displayed in Figs. 4 through 6. Three different environments were chosen to contrast the arrival structure predicted by the model. The first environment assumes an isospeed water column with c=1500 m/s and a constant depth of 100 m. The source depth for this case is 50 m. The second environment also assumes an isospeed water column with c=1500 m/s but uses bathymetry

extracted from the MAB region between the SW 400 Hz source and NW VLA. The third environment uses both bathymetry and sound speed data extracted from the MAB region. For the second and third environments, the source depth is 300 m. In all cases, the source is modeled as a point source with a center frequency of 400 Hz and 100 Hz bandwidth. Also, all three environments assume a homogeneous fluid bottom type with sound speed, density, and attenuation of 1600 m/s, 1.2 g/cm^3, and 0.1 dB/m/kHz`, respectively. Figures 4 through 6 show the arrival structures of the beams as a function of arrival time and arrival angle. In these figures, it is seen that changes to the environment affect the vertical arrival structure at the array. The difference in arrival angle of primary energy is seen in Figs. 4 and 5 due to the upslope bathymetry input into the model. Specifically, energy arriving at grazing is reduced and the largest arrivals are observed near 10°. Next, when the MAB sound speed profile is included, the simple symmetry of arrivals in the previous cases is removed, as seen in Fig. 6. Most of the energy arriving between -10° and 10° is observed to occur within about the first 0.1 s. Between +/- 10° and 15°, the arrivals rapidly stretch over 0.5 s. This is typical of ducted profiles where propagation angles away from grazing encounter faster sound speeds which counter the path lengths. Beyond some angle, however, the increased path length dominates the travel time and arrival times

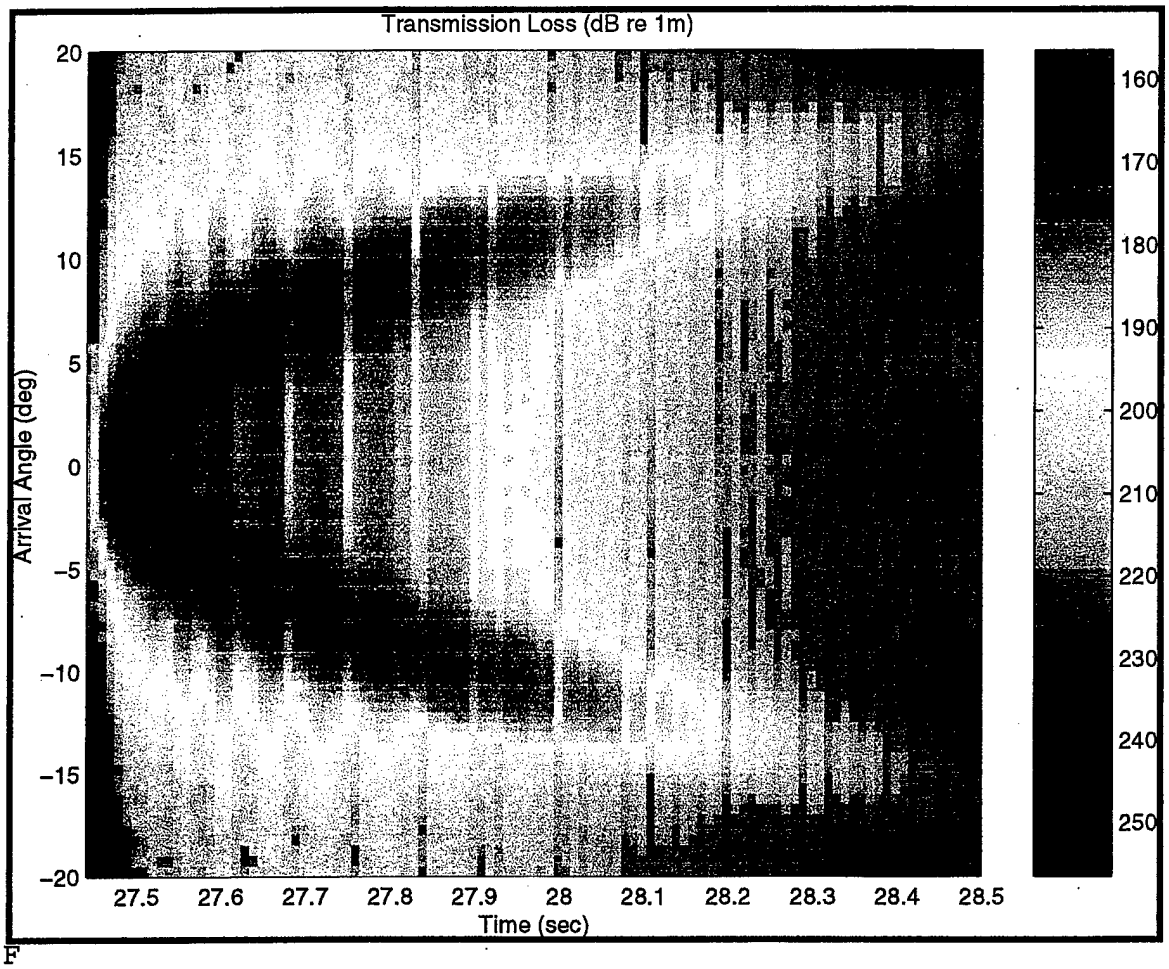

Figure 4: Arrival angle-arrival time display of a simple isospeed, isobath environment.

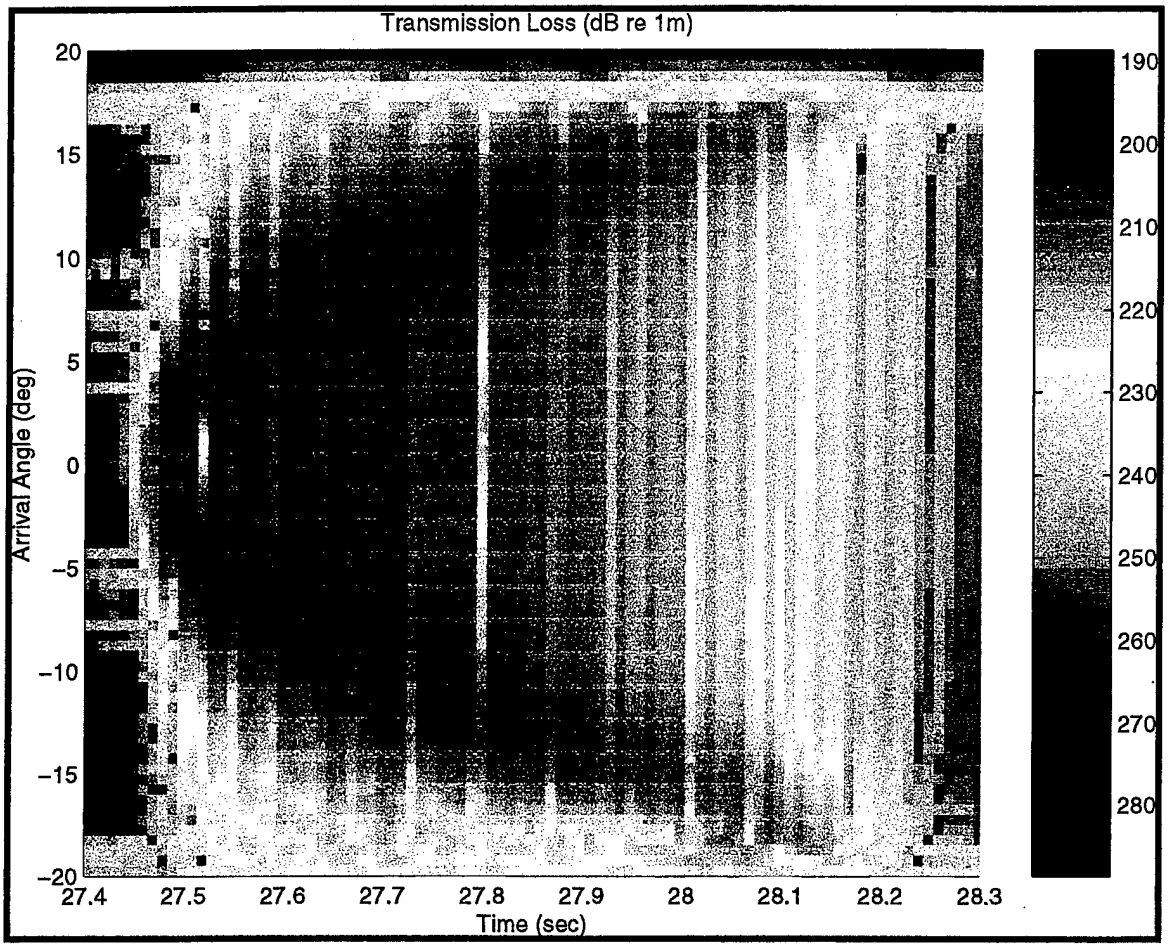

Figure 5: Arrival angle-arrival time display of isospeed environment with the bathymetry of the MAB region.

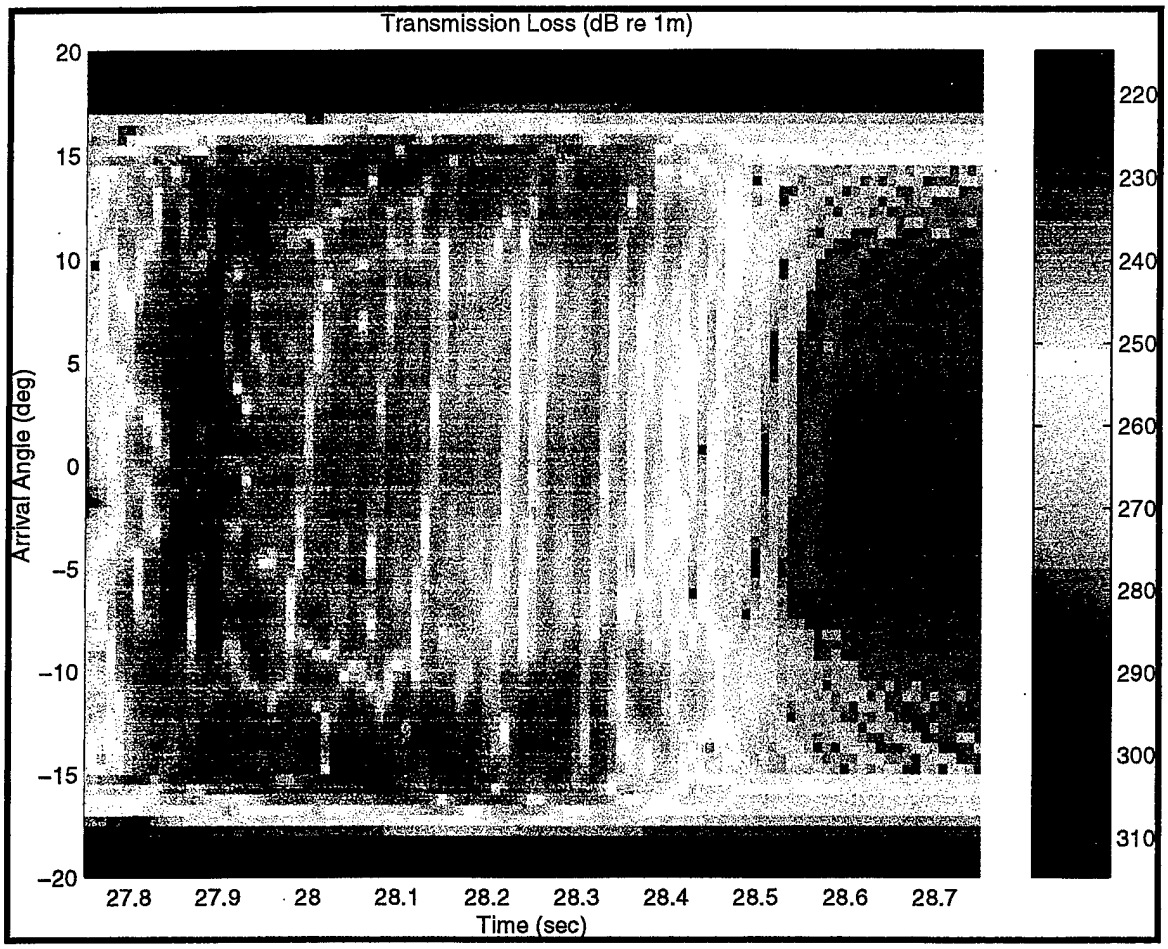

Figure 6: Arrival angle-arrival time display of environment with bathymetry and sound speed profile of the MAB region.

of the energy arriving between -10° and 10° is observed to occur within about the first 0.1 s. Between +/- 10° and 15°, the arrivals rapidly stretch over 0.5 s. This is typical of ducted profiles where propagation angles away from grazing encounter faster sound speeds which counter the path lengths. Beyond some angle, however, the increased path length dominates the travel time and arrival times increase rapidly.

2. Observed Arrival Structures

During the MAB experiment, approximately 90 gigabytes of data was acquired and stored on a telemetry buoy. This data was transferred from the telemetry buoy to 8-millimeter tapes. There were nine disks (01-09) of data available for processing. Of the nine disks, however, there are three gaps in the data due to equipment failures (Heydt, 1996). The longest period without gaps in the data is on disks 07 through 09. These disks contain 3 days of data. To beamform the data, the depth-time matrix was read into the beamformer algorithm. A Hamming filter was used to reduce sidelobes of the signal. The depth-time matrix was then zero padded (increase the number of points in the matrix to a value of 2^N) which prepared the matrix for an FFT. A series of FFT's were performed to transform from time to frequency domain, depth to vertical wavenumber space, vertical wavenumber space to angle, and finally from frequency back to the time domain. The end result is an

identical to Fig. 6. The duration of the arrival is approximately 0.75 seconds, similar to the prediction. The signals peak with early arrivals and drop off sharply to negligible amounts.

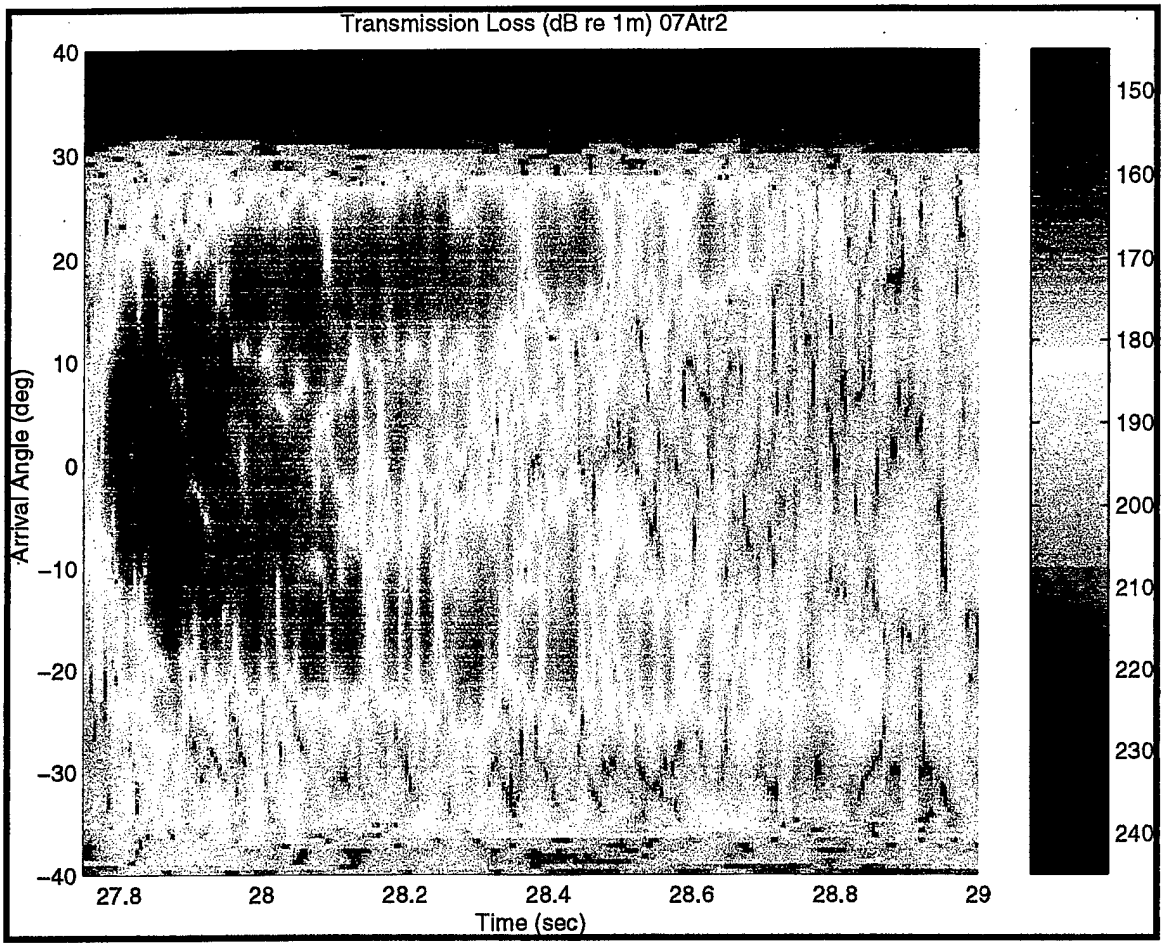

Figure 7: Arrival angle-arrival time display of single SW to NW transmission that has been beamformed.

IV. DATA ANALYSIS

A. SPATIAL COHERENCE

To analyze the spatial coherence of the phones, a single record of the VLA data was examined. The peak correlation of each phone's data with the bottom phone was computed and normalized such that the autocorrelation of the bottom phone was identically one. This calculation was then repeated relative to the top phone. Figures 8 and 9 show the phone to phone peak correlation of phones from bottom to top and top to bottom, respectively. These results show that the signal correlation drops to ~0.5 over a few phones, at ~10 meters in depth. This suggests different multipath arrivals are interacting across the length of the array at slightly different times.

To observe the correlation of the beams, a single transmission was beamformed. After beamforming, the center beam was extracted from the angle-time matrix and the peak correlation with higher angle beams was computed, normalized such that the autocorrelation of the center beam with itself is identically one. Similarly, the 10° and 20° beams were extracted and cross-correlated with higher angle beams. Figures 10 through 12 show these beam to beam correlations. In each case, the correlation begin to rapidly decrease

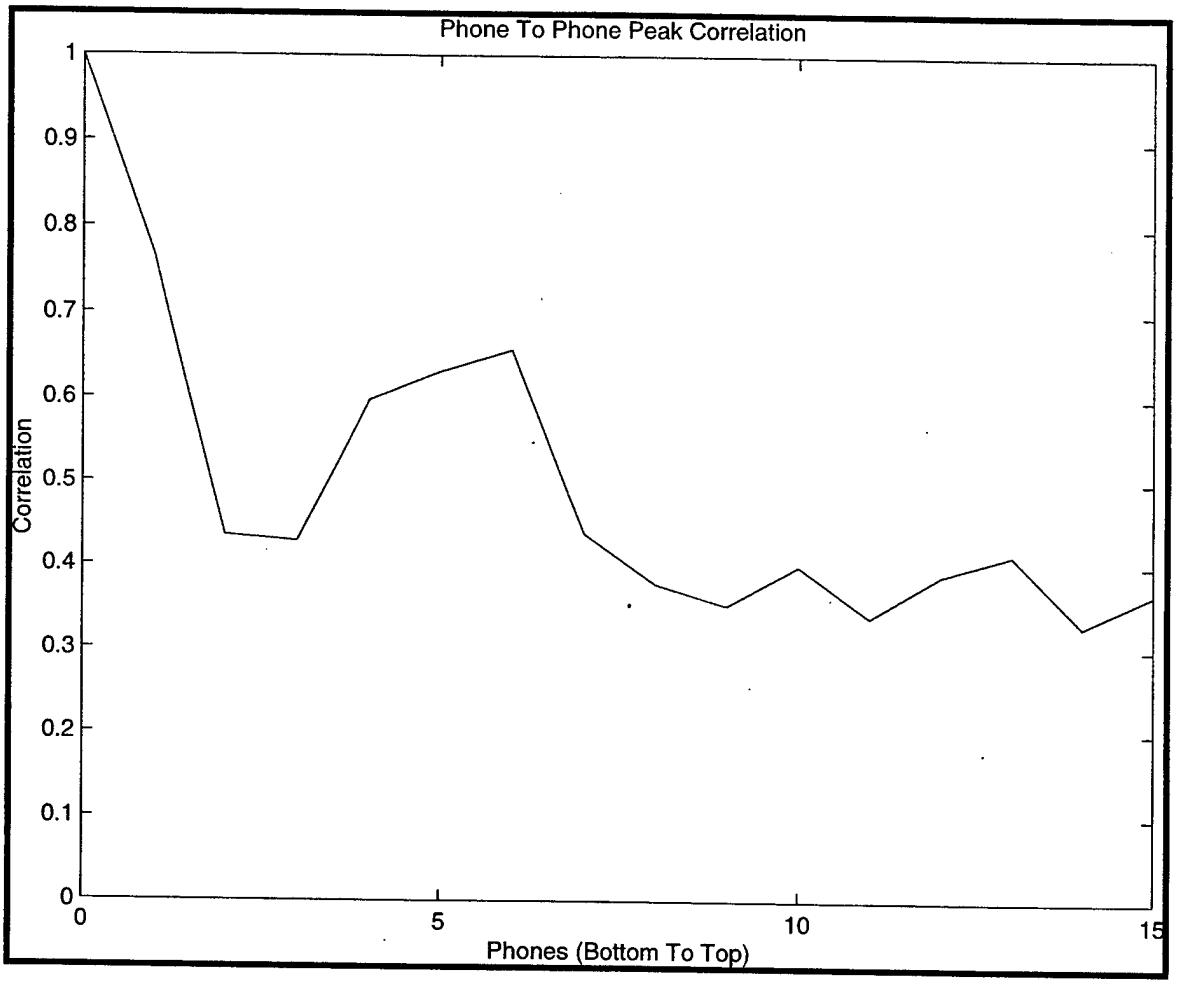

Figure 8: Peak cross-correlation of the phones from bottom to top phone.

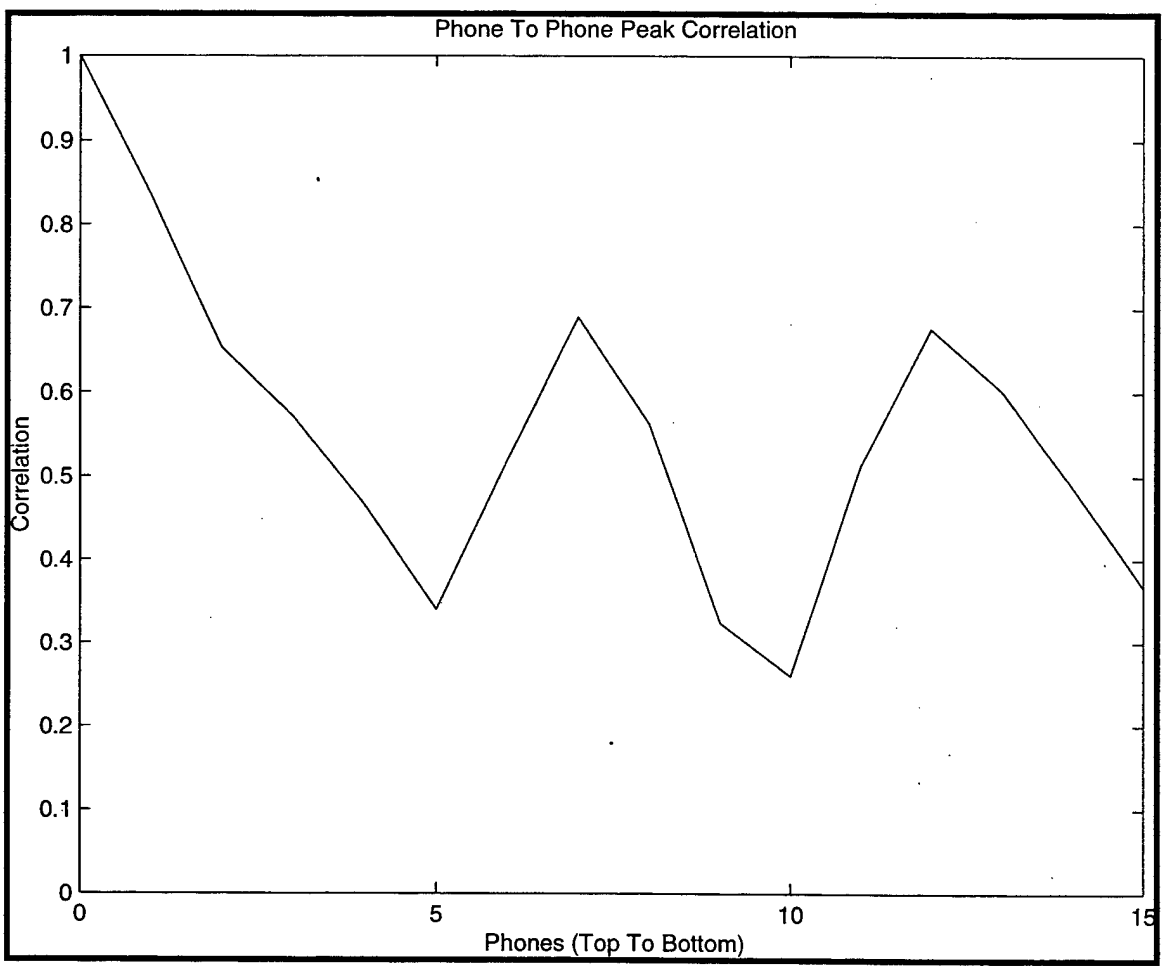

Figure 9: Peak cross-correlation of the phones from top to bottom phone.

above ~27° and drops to a minimum for the beams above ~32°. This is due to a lack of arrival energy beyond this angle and is consistent with a local critical angle between 25° and 30°. With a water column sound speed at the bottom of 1480 m/s, this suggests a local sediment sound speed between 1630 m/s and 1700 m/s. This appears to be a bit large and is possibly due to some side-lobe leakage into angles which do not have any real incident energy. However, direct measurements of geophysical parameters at a nearby site do reveal a sound speed at the top of the sediment of ~1600 m/s with a significant gradient of ~20 m/s/m (Apel et al., 1997).

The highest correlation levels are found in Fig. 10, the cross-correlation of the central beam with higher angles. Because of the upslope nature of the propagation, no significant arrivals are expected near grazing. This appears to be confirmed in the beamformed data displayed in Fig. 7 which indicates dominant arrivals at non-grazing angles. The high correlation values in Fig. 10 are then presumably due to sidelobe leakage from dominant arrivals at higher angles. Figure 11 shows a relatively rapid decorrelation between the 10° beam and higher angles consistent with a significant, unique arrival near 10°. Figure 12 shows a wider correlation peak. However, there does not appear to be a significant amount of energy

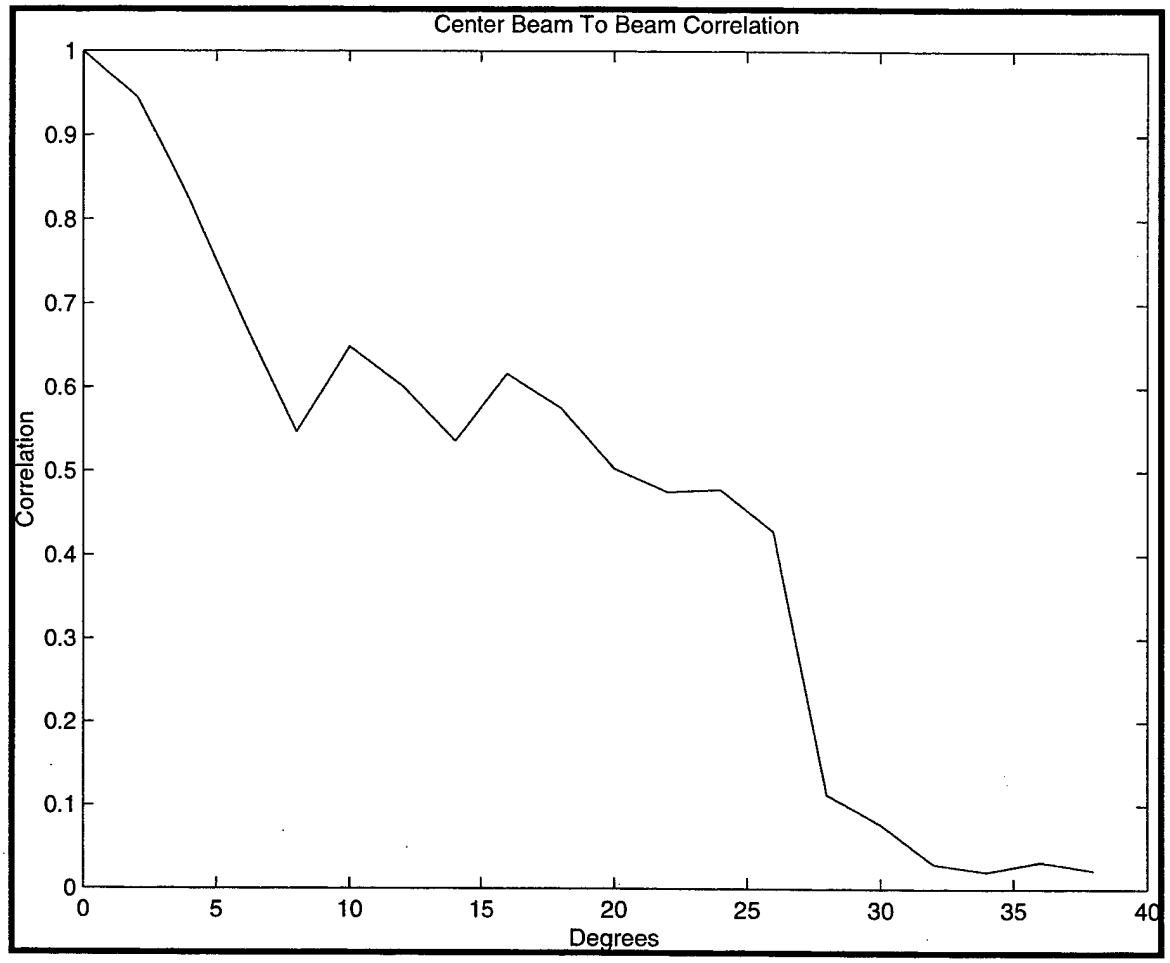

Figure 10: Peak cross-correlation of center beam with beams up to 40°.

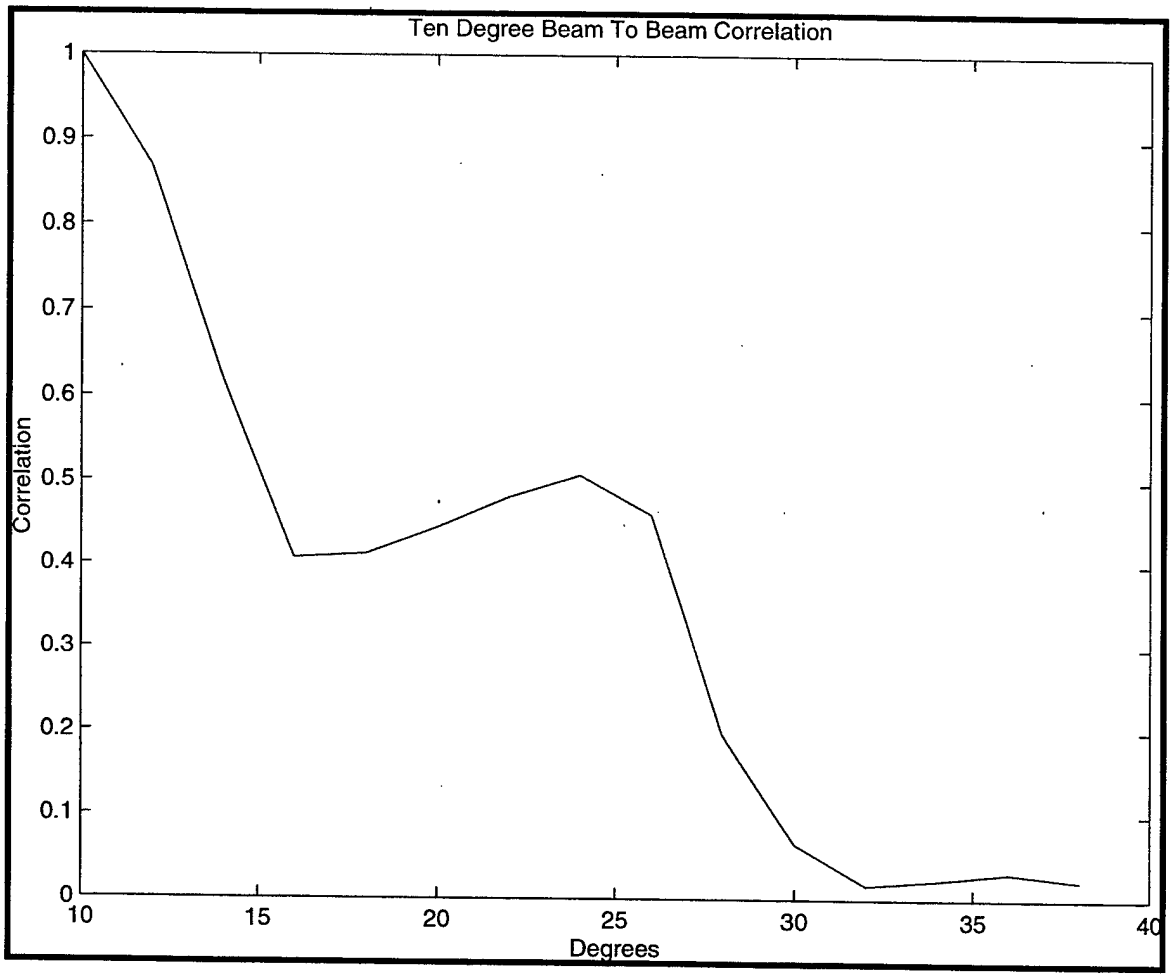

Figure 11: Peak cross-correlation of 10° beam with beams up to 40°.

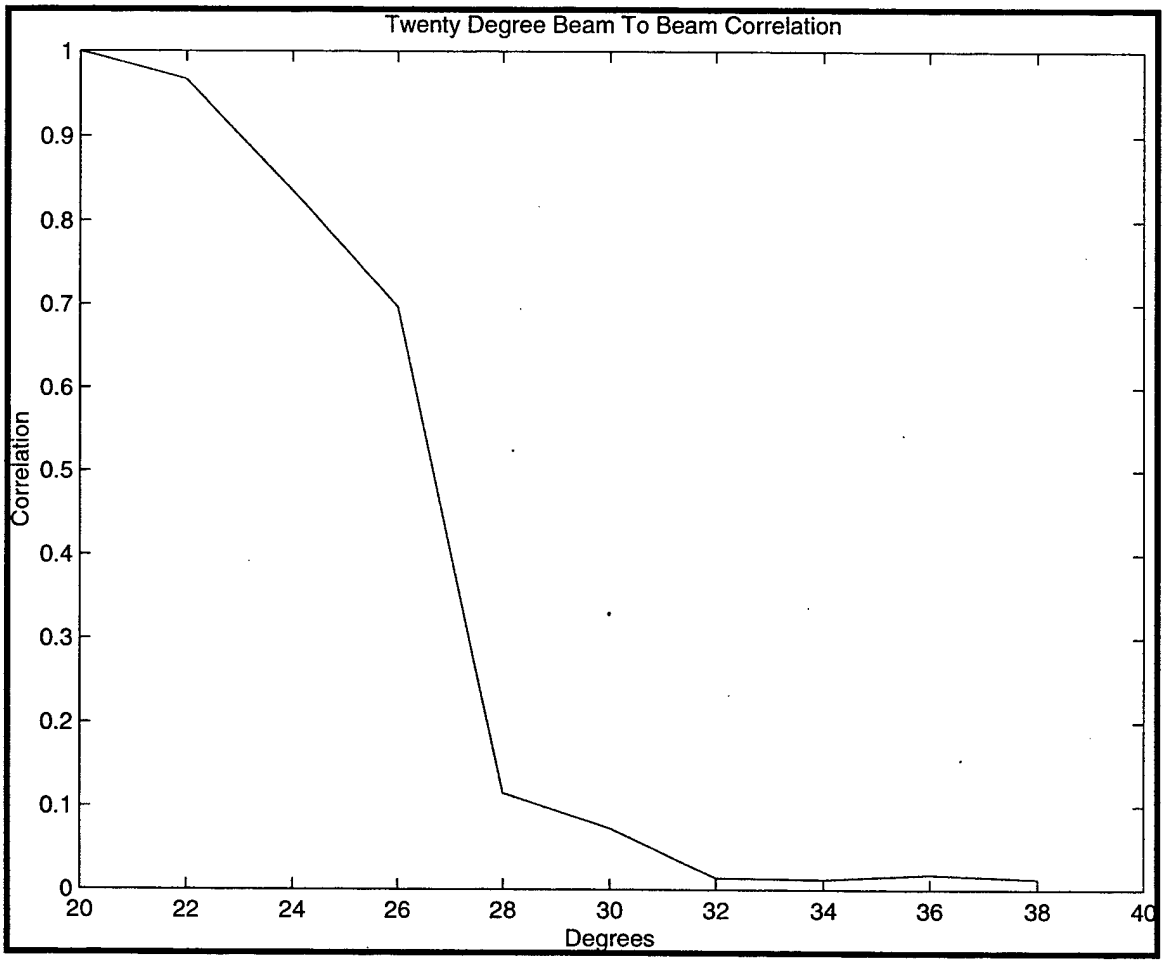

Figure 12: Peak cross-correlation of 20° beam with beams up to 40°.

arriving at 20°, and so the high correlation over ~5° may also be an artifact of sidelobe leakage.

B. TEMPORAL COHERENCE

Temporal coherence of the bottom phones was completed by reading in 3 hours of data (12 transmission records and correlating the center/bottom phone of record 1 with itself and with the center/bottom phone of the other 11 records. The same was done for beams at angles 0°, 10°, and 20°. In all cases, the peak correlation was extracted by shifting the absolute time of each record. Figure 13 shows the temporal coherence of the center and bottom phones. The correlation is seen to drop rapidly from the first ping to the second and then maintain a relatively low value of ~0.5. This indicates that the correlation time of the acoustic transmission is less than our 15 minute sampling. Figure 14 shows the ping to ping correlation of the beams. Again, these plots show a rapid decorrelation of the signal from ping to ping. In order to investigate the actual temporal coherence, it would be necessary to return to the original data before performing the 5-minute averaging.

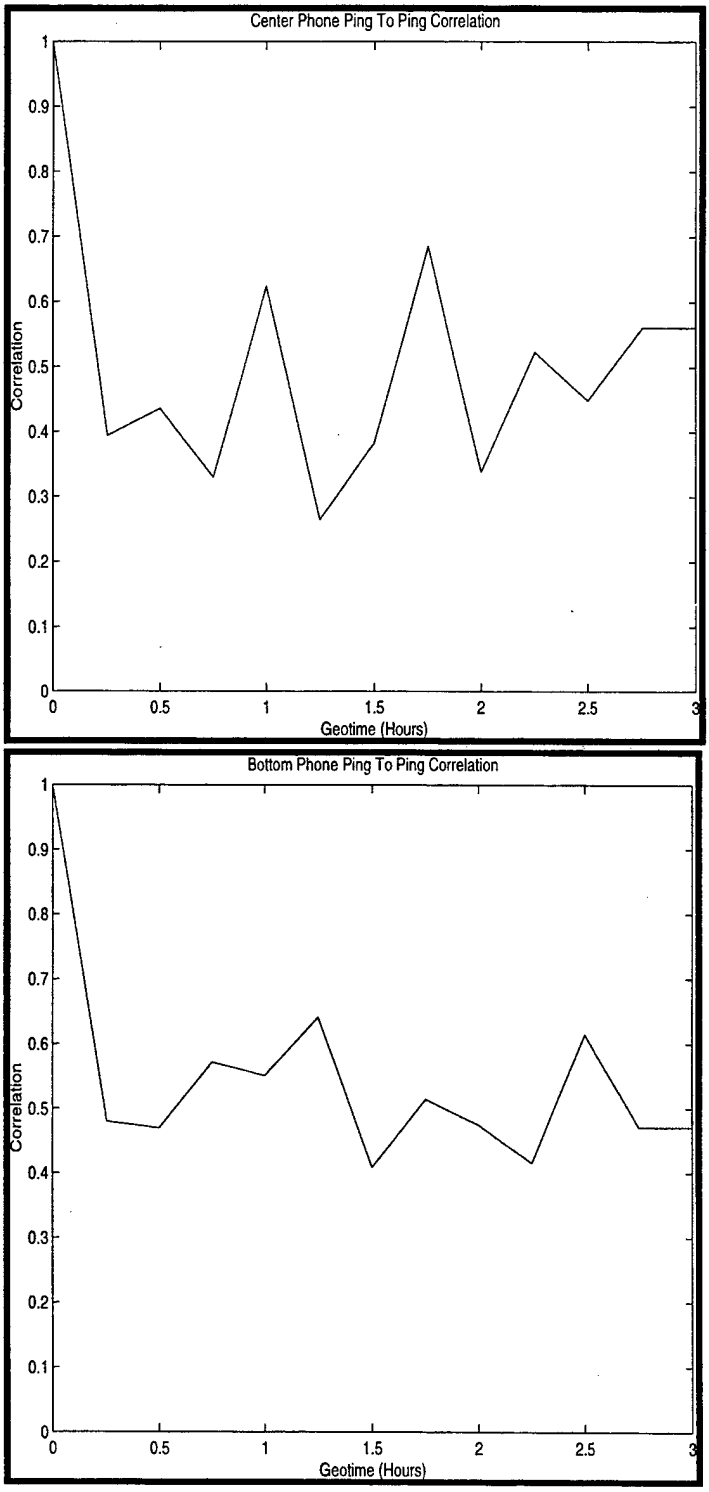

Figure 13: Ping to ping peak correlation of the center phone and bottom phone over a 3-hour period.

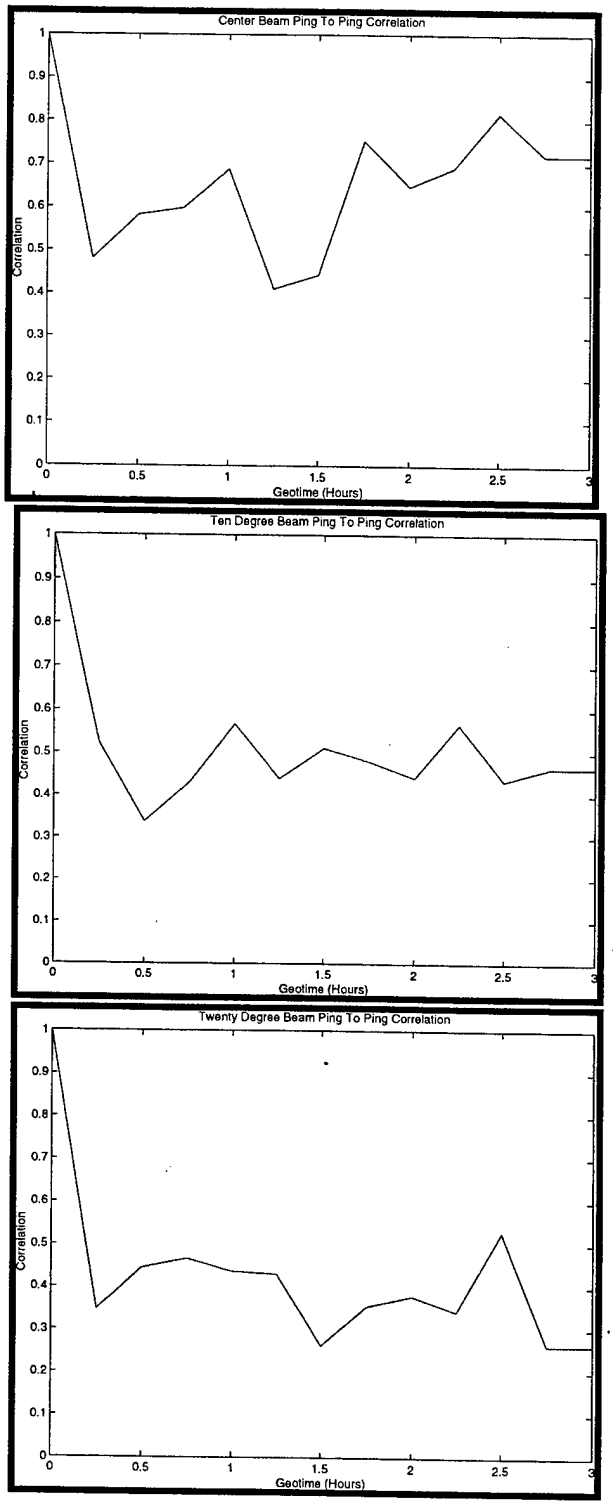

Figure 14: From top to bottom, ping to ping peak cross-correlation of the center, 10°, and 20° beams over a 3-hour period.

C. TIDAL AND FRONTAL TRAVEL TIME INFLUENCES

In Figs. 15 and 16 the arrival structure of the center phone is plotted over a three-hour period (sampled every 15 minutes) and a three-day period (sampled every hour), respectively. Similar plots for other phones and beams have been examined and exhibit the same general characteristics of arrival time versus geotime, and so will not be explicitly presented here. Consistent with the rapid decorrelation computed in the previous section, Fig. 15 shows the large ping-to-ping variation during a three-hour period. Despite these variations in the fine-scale structure over short times, a general trend in the early, peak arrivals can be observed over longer times, as exhibited in Fig. 16. Over the course of three days, the earliest arrival of each record changes from an arrival time of ~27.775 s to ~27.825 s, a difference of ΔT ~0.050 s. In addition, a periodic tidal response of ~12 hours is also observed with peak travel time fluctuations of Δt ~0.030 s.

Let us consider the tidal response first. Physically, the primary influence of the tide on the shelf break front is to push the cold water "tongue" of the front water back and forth over the shelf break. As seen in Fig. 2, this protrusion of cold shelf water occupies roughly 50 m in depth or between ¼ and ½ of the water column beyond the shelf break. In order to estimate the horizontal

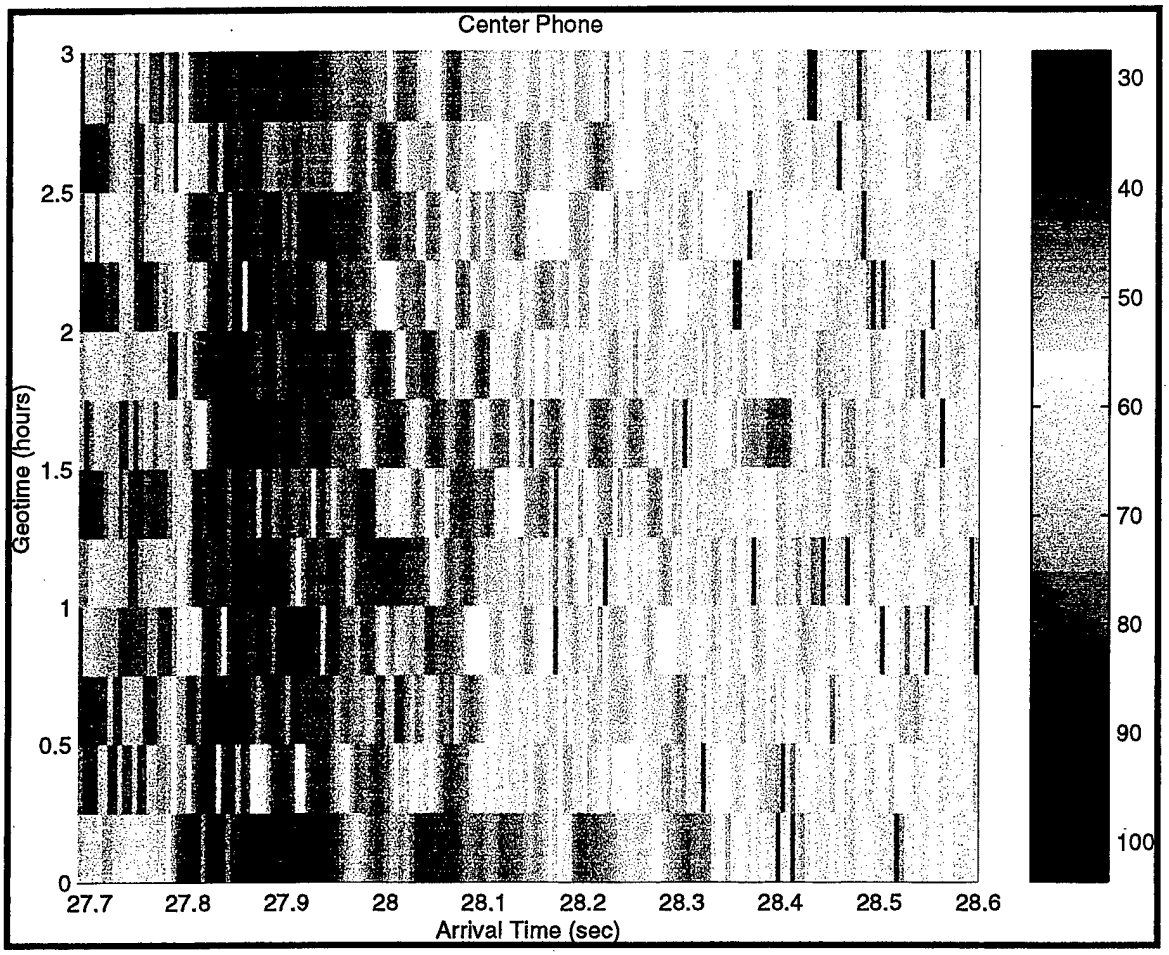

Figure 15: Geotime-arrival time display of arrival structure for center phone over a period of 3 hours.

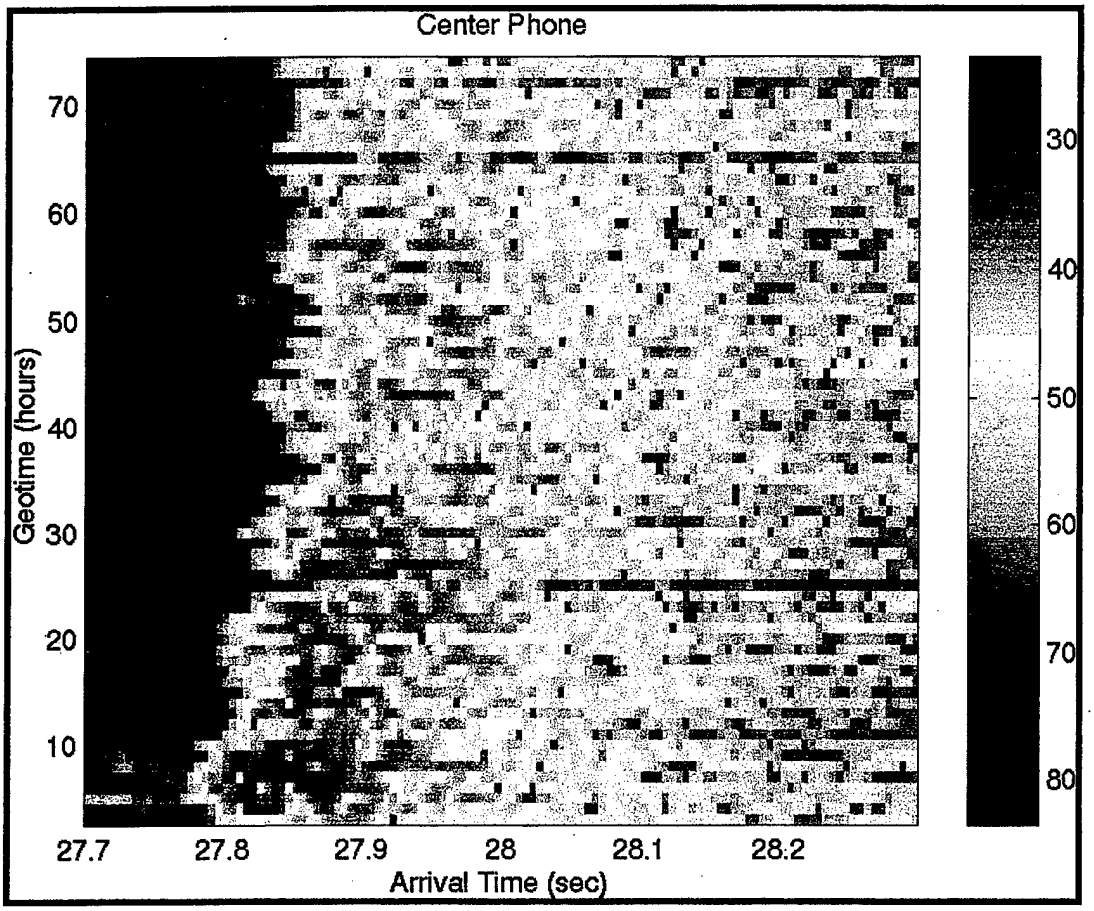

Figure 16: Geotime-arrival time display of arrival structure for center phone over a period of 3 days.

displacement of the front, let us assume a simplistic model in which a section of the cold water front of horizontal extent R_f is replaced by warmer water. Furthermore, we will assume the early arrivals are due to energy propagating at ~10° from grazing, and we will neglect changes in the propagation path. Due to the near grazing propagation, the acoustic path length through this segment is of order ¼ R_f (the ¼ due to the limited vertical extent). If the sound speed over this path changes from $C_{shelf} \approx$ 1475 m/s to C_{warm} ≈1500 m/s, then the travel time will be reduced by an amount

$$\Delta t \approx \frac{1}{4} R_f \left(\frac{1}{C_{shelf}} - \frac{1}{C_{warm}}\right). \qquad (4.1)$$

Given Δt ~0.03 s for the tidal response, the horizontal displacement of the front is then R_f ~10 km. This value is consistent with other oceanographic observations (Chiu, 1997). The change in peak arrival times over the 3-day period examined, ΔT ~0.05 s, was due to a cold shelf water intrusion into the operational area during the experiment Chiu, 1997). Again, let us assume a simplistic model in which all of the water on the shelf, covering the final ~10 km of propagation, was affected by a reduction in sound speed from C_{shelf} ≈1485 m/s to $C'_{shelf} \approx$ 1485 m/s - ΔC_{shelf}. Since this affects the entire path over the shelf, and since the

propagation is still nearly horizontal, we can estimate the change in travel time from

$$\Delta T \approx R_{shelf}\left(\frac{1}{C'_{shelf}} - \frac{1}{C_{shelf}}\right) \approx \frac{R_{shelf}}{C^2_{shelf}}\Delta C_{shelf}. \qquad (4.2)$$

Thus, ΔC_{shelf} ~10 m/s which corresponds to a nearly 2°C change in the water temperature. This appears to be about twice what is expected, and so it may be speculated that the cold water intrusion significantly perturbed the propagation path, increasing both the propagation angles and the total path length. Note that this would be consistent with the observed decrease in arrival amplitudes since higher propagation angles would also generate higher bottom attenuation.

V. CONCLUSION

The Mid-Atlantic Bight experiment was conducted to give the U. S. Navy a better insight into shallow water acoustic propagation near shelf break regions. There was 90 gigabytes of data collected during the experiment. This study involved the signal processing of a small portion of this data using the technique of plane-wave beamforming. The analysis of the beams at the vertical array revealed the following results.

1. The phone to phone peak correlations show that the signal correlation drops to ~0.5 over a few phones, at ~10 meters in depth. This suggests different multipath arrivals are interacting across the length of the array at slightly different times.

2. Beam to beam correlations show a rapid decrease for the beams above ~27°. This is due to a lack of arrival energy beyond this angle and is consistent with a local critical angle of between 25° and 30°. With a water column sound speed at the bottom of ~1480 m/s, this suggests a local sediment sound speed of between 1630 m/s and 1700 m/s. The highest correlation levels are found in the cross-correlation of the central beam with higher angles; however, because of the upslope nature of the propagation, no significant arrivals are expected near grazing.

3. The temporal coherence of the center and bottom phones is seen to drop rapidly from the first ping to the second and then maintain a relatively low value of ~0.5. This indicates that the correlation time of the acoustic transmission is less than our 15-minute sampling. Ping-to-ping correlations of the beams show a rapid decorrelation of the signal. In order to investigate the actual temporal coherence, it will be necessary to return to the original data before performing the 5-minute averaging.

4. Consistent with the rapid decorrelation of temporal coherence, there is a large ping-to-ping variation absorbed during a three-hour period. Despite these variations in the fine-scale structure over short times, a general trend in the early, peak arrivals can be observed over longer times. Over the course of three days, the earliest arrival of each record changes from an arrival time of ~ 27.775 s to ~27.825 s, a difference of ΔT ~0.050 s. In addition, a periodic tidal response of ~12 hours is also observed with peak travel time fluctuations of Δt ~0.030 s.

5. Given Δt ~0.03 s for the tidal response, the horizontal displacement of the front is then R_f ~10 km, which is consistent with other observations. The change in the peak arrival times over the 3-day peroid is due to a cold shelf water intrusion into the operational area of the experiment. A simple analysis suggests ΔC_{shelf} ~10 m/s which corresponds

to a nearly 2°C change in the water temperature. This appears to be about twice what is expected, and so it may be speculated that the cold water intrusion significantly perturbed the propagation path, increasing both the propagation angles and the total path length. This would also be consistent with the observed decrease in arrival amplitudes since higher propagation angles would also generate higher bottom attenuation.

LIST OF REFERENCES

Apel, J. R., M. Badiey, C.-S. Chiu, S. Finette, R. Headrick, J. Kemp, J. F. Lynch, A. Newhall, M. H. Orr, B. H. Pasewark, D. Tielbuerger, A. Turgut, K. V. Heydt, and S. Wolf, "An Overview of the 1995 SWARM Shallow-Water Internal Wave Acoustic Scattering Experiment," *IEEE Journal of Oceanic Engineering*, Vol. 22, No.3, 1997.

Birdsall, T. G. and K. Metzger, "Factor inverse matched filtering," *J. Acoust. Soc. Am.*, 79, 191-221, 1986.

Chiu, C.- S., Department of Oceanography, Naval Postgraduate School, Monterey, CA, Personal Communication, 1997.

Clay, C. S. and H. Medwin, *Acoustical Oceanography: Principles and Applications*, pp. 447-449, New York: John Wiley and Sons, 1977.

Defatta, D. J., G. Lucas and W. S. Hodgkiss, *Digital Signal Processing: A System Design Approach*, pp. 628-649, New York: John Wiley and Sons, 1988.

Hardin, R. H. and F. D. Tappert, "Applications of the Split-Step Fourier Method to the Numerical Solution of Nonlinear and Variable Coefficient Wave Equation," *SIAM Rev 15*, 1973.

Heydt, K. V., Primer-96 VLA Data Information, Woods Hole Oceanographic Institution, Dept of Applied Ocean Physics and Engineering, 1996.

Jensen, F. B., W. A. Kuperman, M. B. Porter, and H. Schmidt, *Computational Ocean Acoustics*, p. 566, New York: American Institute of Physics, 1994.

Munk, W., P. Worcester, and C. Wunsch, *Ocean Acoustic Tomography*, pp. 188-196, New York: Cambridge University Press, 1995.

Pickart, R. S., G. G. Gawarkiewicz, J. F. Lynch, C.-S. Chiu, K. B. Smith, and J. H. Miller, *Endeavor 286 Cruise Summary*: Primer III, 1996.

Smith, K. B. and F. D. Tappert, "UMPE: University of Miami Parabolic Equation Model, Version 1.1" MPL Technical Memorandum 432, San Diego, CA, 1995.

Smith, K. B., J. H. Miller, J. F. Lynch, and C.-S. Chiu, "Shelfbreak Primer Quicklook: Acoustic Observations and Modeling Comparison," Naval Postgraduate School, Monterey, CA, 1996.

Snyder, J., "Undersea Warfare: The Battle Below", Chief of Naval Operations, Surface Warfare Division (N86) Washington, DC, 1997.

INITIAL DISTRIBUTION LIST

		No. Copies
1.	Defense Technical Information Center 8725 John J. Kingman Rd., Ste 0944 Ft. Belvoir, Virginia 22060-6218	2
2.	Dudley Knox Library Naval Postgraduate School 411 Dryer Rd. Monterey, California 93943-5101	2
3	Department Chairman Code PH Department of Physics Naval Postgraduate School Monterey, California 93943-5101	1
4.	Professor Kevin B. Smith Code PH/Sk Department of Physics Naval Postgraduate School Monterey, California 93943-5101	5
5.	Professor Ching-Sang Chiu Code OC/Ci Department of Oceanography Naval Postgraduate School Monterey, California 93943-5101	1
6.	LT Jerry L. Sullivan 343 Davis Street Portsmouth, RI 02871	1
7.	Dr. James F. Lynch Department of Applied Ocean Physics and Engineering Woods Hole Oceanographic Institution Woods Hole, Massachusetts 02543	1
8.	Dr. Jeff Simmen Office of Naval Research 800 North Quincy Street Arlington, Virginia 22217-5660	1
9.	Dr. Ellen Livingston Office of Naval Research 800 North Quincy Street Arlington, Virginia 22217-5660	1